Ground ice in the upper permafrost of the Beaufort Sea Coast of Alaska

Article *in* Cold Regions Science and Technology · August 2013
DOI: 10.1016/j.coldregions.2012.08.002

9 authors, including:

Mikhail Kanevskiy
University of Alaska Fairbanks
93 PUBLICATIONS **1,362** CITATIONS
SEE PROFILE

Y. L. Shur
University of Alaska Fairbanks
119 PUBLICATIONS **3,086** CITATIONS
SEE PROFILE

Chien-Lu Ping
University of Alaska Fairbanks
157 PUBLICATIONS **5,230** CITATIONS
SEE PROFILE

Gunner Michaelson
Sierra College
75 PUBLICATIONS **3,353** CITATIONS
SEE PROFILE

Cold Regions Science and Technology 85 (2013) 56–70

Contents lists available at SciVerse ScienceDirect

Cold Regions Science and Technology

journal homepage: www.elsevier.com/locate/coldregions

Ground ice in the upper permafrost of the Beaufort Sea coast of Alaska

M. Kanevskiy [a,*], Y. Shur [a], M.T. Jorgenson [b,a], C.-L. Ping [c], G.J. Michaelson [c], D. Fortier [d,a], E. Stephani [a], M. Dillon [a], V. Tumskoy [e]

[a] Institute of Northern Engineering, University of Alaska Fairbanks, Fairbanks, AK, USA
[b] Alaska Ecoscience, Fairbanks, AK, USA
[c] Palmer Research Center, Agricultural & Forestry Experiment Station, University of Alaska Fairbanks, Palmer, AK, USA
[d] Département de géographie, Université de Montréal, Montréal, QC, Canada
[e] Department of Geology, Moscow State University, Moscow, Russia

ARTICLE INFO

Article history:
Received 21 January 2012
Accepted 18 August 2012

Keywords:
Permafrost
Ground ice
Cryostructures
Ice content
Ice wedges
Alaska

ABSTRACT

Ground ice in the upper permafrost of the Beaufort Sea coast of Alaska was studied from 2005 to 2008 at 65 field sites located between Point Barrow and the Canadian border. The main terrain units in the studied area include (1) the primary surface of the coastal plain; (2) drained-lake basins; (3) low foothills (yedoma); (4) deltas and tidal flats; and (5) sand dunes. Wedge ice is the main type of massive ground ice, and ice-wedge polygons occurred on nearly all land surfaces. The volumetric content of wedge ice for the area varies from 3% to 50% between various terrain units with average value of about 11% for the entire coast. The highest content of wedge ice (about 50%) is typical of yedoma terrain, which occurred in a small segment at the coast of the Camden Bay. At the primary surface of the western region of the Arctic Coastal Plain, wedge-ice content reached almost 30%, with an average value of about 14%. Slightly smaller values were estimated for the primary surface of the eastern region of the Arctic Coastal Plain and for old drained-lake basins. Other types of massive ground ice included thermokarst-cave ice, ice cores of pingos, and a rare occurrence of folded massive ice at Barter Island. The content of segregated ice in organic and mineral soils between ice wedges was very high at most of the study sites. The total average volumetric ice content (due to wedge, segregated, and pore ice) for the whole area was 77%, ranging from 43% in eolian sand to 89% in yedoma.

1. Introduction

Quaternary sediments of the coastal region of northern Alaska contain a high amount of ground ice of different types (Black, 1983; Brown and Sellmann, 1973; Ferrians, 1988; Hussey and Michelson, 1966; Jorgenson et al., 2003; Jorgenson, 2011; Kanevskiy et al., 2008, 2011b; Leffingwell, 1915, 1919; Ping et al., 2011; Pullman et al., 2007; Shur and Jorgenson, 1998). In the adjacent areas of the Beaufort Sea coast of Canada, ground ice was described by Rampton and Mackay (1971), Pollard and French (1980), Harry et al. (1988), Pollard (1990), Mackay and Dallimore (1992), Burn (1997), Mackay (1997), French (1998), Kokelj et al. (2002), Kokelj and Burn (2005), Murton (2005, 2009), Burn and Zhang (2009), and Morse et al. (2009). These studies indicate that the terrain characteristics and cryogenic structure of soils in the coastal region of the Canadian Arctic and Alaska have many similarities. However, numerous bodies of tabular massive ice have been described in Canada, while in Alaska folded massive ice bodies have been observed only at Barter Island (Jorgenson and Shur, 2008; Kanevskiy et al., 2008, 2011b).

Leffingwell (1915, 1919) made the first systematic study of ground ice in the Arctic Coastal Plain of Alaska. His pioneering work on the nature and properties of wedge ice had been unmatched for almost 50 years and remains one of the most important studies in permafrost science. Contemporary research of ground ice on the Arctic Coastal Plain began with works by Black (1952, 1983) and Brown (1967, 1969). Black (1952) studied ice-wedge polygons and the frequency of thermal cracking of permafrost and ice-wedge formation. Brown (1969) provided data on the chemical composition of ice wedges. Brown and Sellmann (1973) found that the volume of ground ice is commonly up to 80% in the upper 2 to 4 m of permafrost, in large part due to the presence of interstitially segregated ice. Jorgenson et al. (1998) and Shur and Jorgenson (1998) described impact of terrain evolution in the Colville River Delta on ground-ice accumulation and the soil cryostructure formation. Jorgenson and Shur (2007) studied the formation of ground ice in drained-lake basins. Pullman et al. (2007) evaluated potential thaw settlement of soils. Almost all works on permafrost structure and properties were conducted in the western region of the Beaufort Sea coast of Alaska (BSCA). Information on ground ice in the eastern

* Corresponding author at: Institute of Northern Engineering, University of Alaska Fairbanks, 237 Duckering Bldg., P.O. Box 755910 Fairbanks, AK 99775-5910, USA. Tel.: +1 907 474 1905.
E-mail address: mkanevskiy@alaska.edu (M. Kanevskiy).

0165-232X/$ – see front matter © 2012 Elsevier B.V. All rights reserved.
http://dx.doi.org/10.1016/j.coldregions.2012.08.002

region of the BSCA has not been greatly improved after Leffingwell (1919).

Evaluation of types and volumes of ground ice in the upper permafrost of the BSCA is important for engineering and environmental evaluations and is essential to quantification of the fluxes of carbon and sediments into the Beaufort Sea and to understanding the response of permafrost terrain to climate change. Upper permafrost to a depth of 2 to 3 m is usually ice-rich and has a specific set of cryostructures (patterns in frozen soil formed by segregated ice) that differs greatly from underlying permafrost (Brown and Sellmann, 1973; Pollard and French, 1980; Shur, 1988a,b). This part of permafrost is the first to be affected by climate warming and various environmental impacts including fire and development, which lead to an increase in thickness of the active layer and thawing of the upper permafrost. Thaw settlement associated with thawing of the upper part of permafrost is detrimental to roads and airfields. Upper permafrost is a storage for organic matter and a source of carbon (Ping et al., 2008b, 2011).

Our 2005–2008 study was a part of a project on the evaluation of the carbon stock in the upper permafrost of the BSCA (Ping et al., 2011). The lack of quantification of volume of ground ice obscures an assessment of soil carbon stocks (Ping et al., 2008b, 2011) and the flux of carbon from soil affected by coastal erosion (Jorgenson and Brown, 2005). The recent increase in coastal erosion (Jones et al., 2009; Jorgenson and Brown, 2005) has intensified the release of organic carbon from eroded soil (Jorgenson et al., 2003; Ping et al., 2008b, 2011).

Ground ice is one of the dominant factors affecting the rate of coastal erosion in the Arctic. Jorgenson and Brown (2005) found that the volume of segregated ice and wedge ice has a greater effect on erosion rates than the exposure of a shore to large, open water fetch. Similarly, Shur et al. (2002) found that high ice content increases the rate of thermal denudation of soil from bluffs, and that the denudation rate of exposed ice-rich permafrost can be greater than the average rate of thermal erosion.

We have studied abundance and distribution of ground ice in the upper permafrost through sampling and testing upper permafrost at 65 sites distributed along the entire 1957-km-long Beaufort Sea coast of Alaska from Point Barrow to the Canadian border (Fig. 1). Specific objectives of our ground-ice study were to classify and describe ground-ice characteristics, quantify the volume of massive, pore, and segregated ice in the upper permafrost to a depth of 2 to 3 m, and evaluate the distribution of ground ice in relation to terrain units along the BSCA.

2. Study area

The coastal part of the Arctic Coastal Plain is a lowland with the flat surface. Most bluffs along the BSCA vary in height between 2 and 4 m. Only at several locations the bluffs rise up to 10 m above the sea level. Several rivers and numerous creeks run through the Arctic Coastal Plain and form their deltas there.

BSCA belongs to the Arctic climatic zone of Alaska (Selkregg, 1975). Freezing index along the coastal plain is practically uniform and reaches about 4800 degree-days below 0 °C. Thawing index decreases from east to west from 290 degree-days above 0 °C (Barter Island) to 240 degree-days above 0 °C (Barrow). Mean annual air temperature is −11.3 °C at Prudhoe Bay, −12.3 °C at Barrow, and −12.4 °C at Barter Island. Mean annual precipitation does not exceed 200 mm.

The surficial deposits of the main surface of the BSCA are presented by Quaternary sediments of different origins comprising the Gubik Formation (Black, 1964; Brigham, 1985; Dinter et al., 1987; Gryc et al., 1951; Rawlinson, 1993). According to engineering-geologic maps of northern Alaska (Carter, 1983a; Carter and Galloway, 1985; Carter et al., 1986; Williams and Carter, 1984; Williams et al., 1977), surficial deposits in the coastal area have mostly marine origin. Marine sediments (mainly silt and clay) include some glacial erratics. The marine deposits are attributed to several Quaternary transgressions, which have been identified for coastal regions in Alaska (Brigham-Grette and Carter, 1992; Hopkins, 1967; O'Sullivan, 1961; Sellmann and Brown, 1973). These deposits have been modified in part by thermokarst, lacustrine, and paludification processes, resulting in an abundance of lake-basin deposits that mantle a significant part of the coastal plain. Lakes can form as water-filled depressions or as thermokarst lakes and lake basins typically undergo multiple stages of evolution (Jorgenson and Shur, 2007). Mineral soils in the mature drained-lake basins are usually overlain by a layer of peat. Other surficial deposits include eolian, alluvial, and deltaic silts and sands. A possible occurrence of glacial deposits at

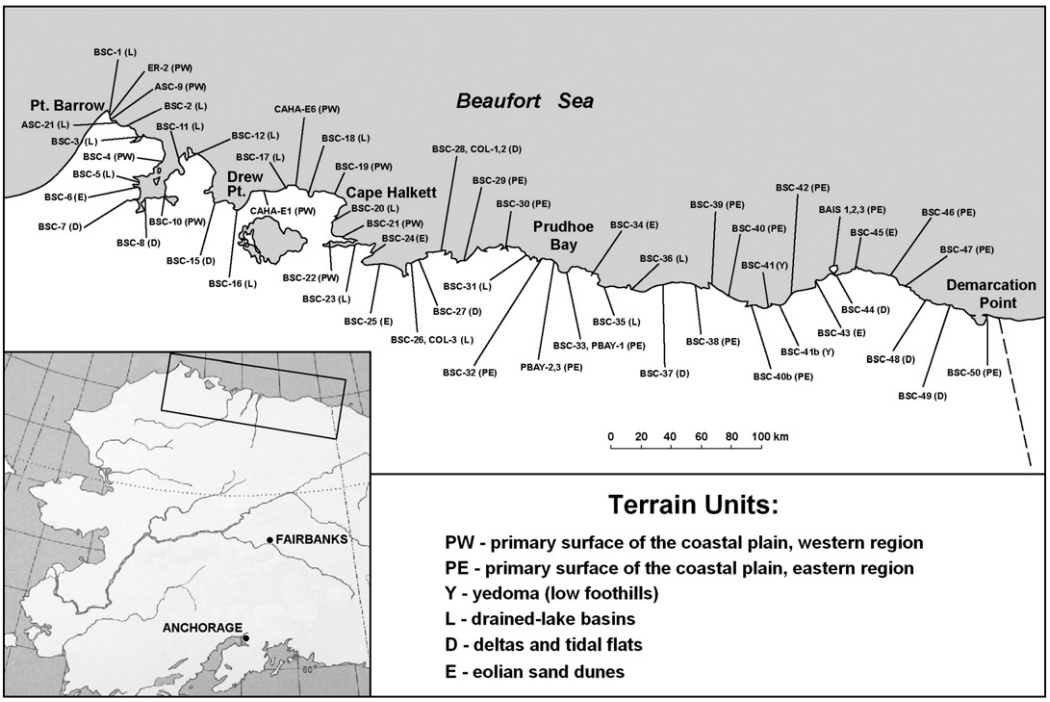

Fig. 1. Location of field sites studied in 2005–2008 along the Beaufort Sea coast from Point Barrow to the Canadian border.

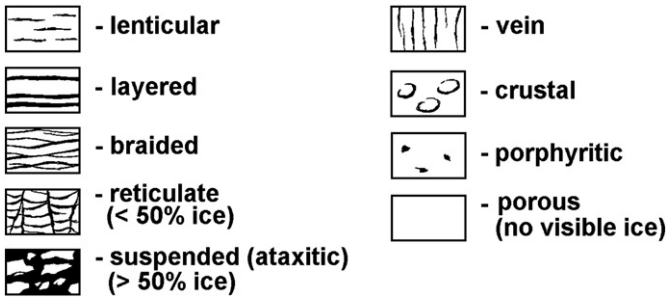

Fig. 2. Main types of cryostructures of mineral soils (ice is black).

the BSCA has been recently discussed by Shur et al. (2001), Jorgenson and Shur (2008), and Kanevskiy et al. (2008, 2011b).

Contemporary sedimentation takes place in deltas and at barrier islands. Most of the mainland coast is affected by active erosion (Reimnitz et al., 1988). Jorgenson and Brown (2005) distinguished five basic coastal types along the 1957 km BSCA: exposed bluffs (16% of the total BSCA length), bays and inlets (12%), lagoons with barrier islands (28%), tapped lake basins (9%), and deltas (35%). Rates of coastal erosion are extremely variable: the mean annual retreat rate varied from 0.7 m/year for lagoons to 2.4 m/year for exposed bluffs. At several sites, the rate of erosion reached 17 m/year (Jorgenson and Brown, 2005). An analysis of aerial photography for 60 km segment of the Alaskan Beaufort Sea coast between Drew Point and Cape Halkett (Jones et al., 2009) revealed that mean annual erosion rates for different time periods reached 6.8 m/year (1955 to 1979), 8.7 m/year (1979 to 2002), and 13.6 m/year (2002 to 2007). Overall, the long-term estimate of the average erosion rate is 1.0 ± 0.7 m/year for the entire BSCA including deltas (Ping et al., 2011).

Permafrost at the BSCA is continuous; its thickness exceeds 200 m and reaches its maximum of 600 m in the Prudhoe Bay area (Brown and Sellmann, 1973; Jorgenson, 2011; Jorgenson et al., 2008; Lachenbruch et al., 1988). The active layer depth varies depending on local conditions from about 20 cm in organic material to more than 100 cm at poorly vegetated sand dunes. Mean annual permafrost temperature at the depth of zero annual amplitude varies depending on local conditions from about −10 °C to −5 °C (Smith et al., 2010), but can be close to 0 °C under wide shallow lakes. If the water depth is greater than critical value (about 1.5 m for this region), mean annual bottom temperature exceeds 0 °C and a closed talik develops. Permafrost temperature in deep boreholes over the last 20 years has increased up to 2.7 °C (Brown and Romanovsky, 2008; Osterkamp and Jorgenson, 2006; Smith et al., 2010).

The study sites (Fig. 1) represent five major terrain units, which were distinguished on the basis of geomorphology and surficial geology:

(1) Primary surface of the Arctic Coastal Plain, labeled in Fig. 1 as PW — western region (predominantly silty deposits) and PE — eastern region (predominantly gravelly sand).
(2) Low foothills formed by yedoma (syngenetic permafrost — ice-rich silt with large ice wedges), labeled in Fig. 1 as Y.
(3) Drained-lake basins (predominantly silty deposits), labeled in Fig. 1 as L.
(4) Deltas and tidal flats (predominantly silt and sand), labeled in Fig. 1 as D.
(5) Eolian sand dunes, labeled in Fig. 1 as E.

3. Methods

Field studies included descriptions of soils and ground ice in exposures and boreholes. The descriptions of soil cryogenic structure were based on classification of cryostructures (specific types of cryogenic structure which can be defined as patterns formed by inclusions and lenses of pore and segregated ice in the frozen soil) for the Arctic Coastal Plain by Shur and Jorgenson (1998) and several other classifications (Gasanov, 1963; Katasonov, 1969; Melnikov and Spesivtsev, 2000; Murton and French, 1994; Ping et al., 2008a; Zhestkova, 1982). The main cryostructures of mineral soils are shown in Fig. 2.

Field descriptions of frozen soils were accompanied by photographs and sketches. Drilling was performed with a SIPRE corer (7.5 cm diameter), and depths of boreholes typically reached 2 to 3 m. At exposures, soil samples were obtained with battery powered hand drills equipped with a hole saw. The height of studied exposures was 1.5 to 4 m for the majority of field sites. The highest permafrost exposures were studied at McLeod Point (7 m above the sea level) and Barter Island (10 m above the sea level). At most sites, soil samples were obtained every 20 to 30 cm for laboratory analysis of moisture content and bulk density. Volumes of frozen samples were determined in the field by measuring the length and diameter of the cores. The ice content of soil was determined from an initial weight of soil in frozen state and after oven-drying (90 °C, 72 h). Both gravimetric and volumetric water contents were calculated for borehole cores and samples extracted from the exposures. Volumetric ice content was evaluated for 339 samples of frozen soils obtained from 56 sites.

Estimation of the wedge-ice volume was based on the assumption that the cross-section of ice wedges has a shape of an isosceles triangle, which is typical of the epigenetic ice wedges that prevail in the study area, and all polygons are square. Such an approach allows calculation of wedge-ice volume through the volume of truncated pyramids representing the soil block framed by ice wedges (Vtyurin, 1975). Volumetric wedge-ice content (WIC) was calculated according to Eq. (1):

$$\mathrm{WIC} = \frac{VPB - VS}{VPB} = 1 - \frac{1}{3}\frac{H\left(A^2 + AB + B^2\right)}{A^2 H} = 1 - \frac{A^2 + AB + B^2}{3A^2}, \quad (1)$$

where $VPB = A^2H$ — volume of polygonal block with a side length A and height H; $VS = 1/3(A^2 + AB + B^2)H$ — volume of soil block forming a truncated pyramid with base side length A and top side length $B = A - C$, where C — the width of ice wedge.

Wedge-ice volume was estimated for the upper layer of permafrost containing ice wedges, which was not thicker than 3 to 4 m for the majority of study sites. The active layer thickness was not taken into account. Our charts developed for estimation of wedge-ice volume for different dimensions of wedges and polygons based on Eq. (1) are shown in Fig. 3. High variability in shape and dimensions of polygons and ice wedges, and occurrence of wedges of different generations (which was observed at the majority of field sites) somewhat obscure estimation of wedge-ice volume. Although approximate, this estimation shows the difference between wedge-ice volumes for sites with different average dimensions of polygons and ice wedges.

An average size of ice wedges for study sites was estimated in the field. An average size of polygons was estimated from satellite or aerial photographs. To find an average polygon area, we calculated the total number of whole (complete) polygons and one-half of the number of incomplete polygons, located within 100 × 100 m^2 areas adjacent to our field sites. For estimation, the average size of polygons was considered equal to a square root of the average polygon area. Satellite images and aerial photographs were acquired through Internet resources such as Google Earth and the Geographic Information Network of Alaska (GINA), University of Alaska website (http://www.gina.alaska.edu/).

Total volumetric ice content (TVIC), which includes wedge ice, segregated ice, and pore ice, was calculated according to Eq. (2) (Grechishchev and Shur, 1990):

$$TVIC = \mathrm{WIC} + SIC(1 - \mathrm{WIC}), \quad (2)$$

where WIC — volumetric wedge-ice content, unit fraction; SIC — volumetric ice content of soils between ice wedges, unit fraction.

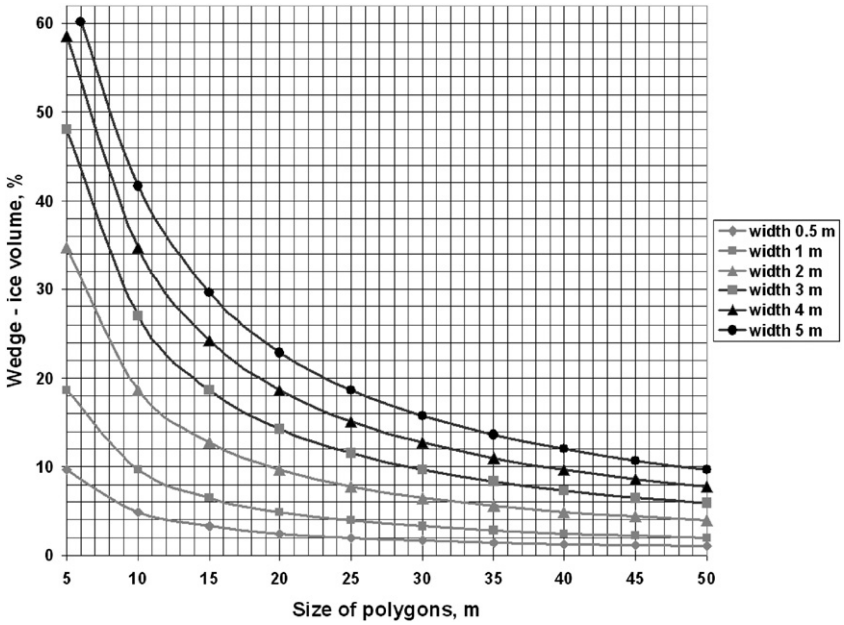

Fig. 3. Content of wedge ice with size of polygons and width of epigenetic ice wedges.

4. Results and discussion

4.1. Classification and characteristics of ground ice

4.1.1. Massive ice

The four main types of massive ground ice occurring along or near the Beaufort Sea shore include (1) ice wedges, (2) thermokarst-cave ice, (3) ice cores of pingos, and (4) folded massive ice.

Wedge ice was by far the most common type of massive ground ice. Ice-wedge polygons occurred nearly everywhere. Low-centered polygons surrounded by ridges are typical for aggrading stages of wedge-ice formation (Shur, 1977; Shur and Jorgenson, 1998), while high-centered polygons indicate stable or partly degraded wedges. The width of wedges in the study area varied from several centimeters to more than 5 m. The tops of ice wedges usually were located no deeper than 10 to 20 cm beneath the permafrost table. The vertical extent of wedges usually did not exceed 4 m, and at many sites they penetrated deeper than contemporary sea level.

Thermokarst-cave ice, which forms from the freezing of water in underground cavities, was frequently observed within and next to ice wedges in the exposed coastal bluffs. Its maximum thickness at our field sites reached up to 120 cm and its visible lateral extent reached up to 5 m. The term *thermokarst-cave ice* was suggested by Shumskii (1959) for massive ice formed by the freezing of water trapped in underground cavities that were cut in permafrost by running water. In Canada, this type of ice was described as *pool ice* by Mackay (1997, 2000).

Ice in pingos was not observed at our study sites, but more than 1000 pingos have been identified on the Arctic Coastal Plain in Alaska (Carter and Galloway, 1979; Ferrians, 1988; Jones et al., 2012). Most pingos are located mainly near Harrison Bay and Prudhoe Bay at some distance from the seashore. Large bodies of folded massive ice of a presumably glacial origin were found recently in the eastern region of the BSCA in a 2-km-long section of coastal bluff at Barter Island (Jorgenson and Shur, 2008; Kanevskiy et al., 2008, 2011b).

The volumes of thermokarst-cave ice, pingo ice, and folded massive ice are much smaller than the volume of wedge ice, and they were not considered in estimations of ground ice contents at the BSCA.

4.1.2. Cryostructures

Six main cryostructures observed at the sampling sites include ataxitic, reticulate, layered, crustal, porous, and organic-matrix (Fig. 4).

Ataxitic (suspended) cryostructure was the most common cryostructure of upper permafrost in the study area, especially in silt and clay (Fig. 4A). This cryostructure consists of an ice matrix with isolated soil aggregates (blocks) suspended in ice. Volume of visible ice in soil with ataxitic cryostructure exceeds 50%, and thicknesses of ice lenses between soil aggregate vary from several millimeters to several centimeters. The soil aggregates had various shapes (angular, sub-angular, platy, sometimes round) and orientation (horizontal, chaotic, or inclined). In the study area, the ataxitic cryostructure very often had a chaotic orientation of mineral blocks (Fig. 4A). The thickness of sediments with ataxitic cryostructure generally varied from 0.5 m to 2 m and occasionally exceeded it. In the shaft of a permafrost tunnel excavated at Barrow in the 1960s (Brown, 1965; Meyer et al., 2010), the thickness of silt with ataxitic cryostructure was about 2 m (Fig. 5).

Reticulate cryostructure is characterized by multidirectional ice lenses usually less than 10 mm thick surrounding mineral blocks (Fig. 4B). This cryostructure was typically observed in silt, clay, silty sand, and sometimes in organic soil. Similar to ataxitic cryostructure, the mineral blocks of soil with reticulate cryostructure had various shapes (angular, sub-angular, platy, sometimes round) and orientation (horizontal, chaotic, sometimes inclined). A gradual transition from reticulate to ataxitic cryostructure was frequently observed.

Layered cryostructure, as well as lenticular and braided cryostructure, is characterized by parallel ice lenses. These cryostructures were observed in the study area in silt, clay, silty sand, and sometimes in organic soil, but they were not as common as ataxitic and reticulate cryostructures. Sometimes these cryostructures occurred together (Fig. 4C). Thicknesses of ice lenses are typically less than 10 mm, but occasionally they can reach several centimeters.

Crustal cryostructure is defined by ice films covering gravel particles. Although typical of gravelly soils, ice crusts were observed around inclusions of organic matter (e.g., fragments of wood). Usually, ice crust thickness was 1 to 2 mm; occasionally, it reached 10 to 15 mm. Crustal cryostructure was frequently accompanied by porous cryostructure, especially in gravelly sands. Fig. 4D shows cryostructure, transitional from crustal to suspended.

Porous cryostructure is characterized by the presence of ice limited to the pore space within the soil matrix and often is not visible (Fig. 4E). It was mostly observed in sandy soils. Sometimes this cryostructure was combined with porphyritic (porous visible) cryostructure, which is characterized by random inclusions of visible ice that fills large pores.

Organic-matrix cryostructure typical of organic soils is controlled by the organic fibers in the soil and can be ice-rich (organic-matrix suspended cryostructure) or relatively ice-poor (organic-matrix porphyritic cryostructure) (Fig. 4F). This cryostructure was abundant in the organic-rich surface horizons at many of the sites. Despite very high moisture content, the amount of visible ice in organic soils is often very small. As a result, thaw settlement of organic soil without external load is usually much smaller than thaw settlement of ice-rich mineral soils with similar volumetric ice content although it should be considerable for engineering projects (Burgess and Smith, 2003). With the external load, thaw settlement of organic soils is very high (Kanevskiy et al., 2012).

4.2. Ground ice in main terrain units

Properties of the upper permafrost such as occurrence of massive ice, cryogenic structure, volumetric content of massive ice, ice content of soil between ice wedges, and the total volume of ice were analyzed in relation to the main terrain units (Table 1 and Fig. 6). In the following sections, we discuss the dominant characteristics of the massive and segregated ice in relation to the main terrain units, including terrain characteristics, peat horizons, polygon size, wedge-ice volume, dominant cryostructures, volumetric ice content of soils, and total ice content (including wedge ice, segregated, and pore ice).

4.2.1. Primary surface of the Arctic Coastal Plain

The primary surface of the Arctic Coastal Plain is formed by a combined set of deposits that have not been reworked by recent lacustrine processes (Black, 1983). The polygenetic deposits presented by silty sand and gravel are typical for the eastern region of the coastal plain, and silt and silty clay dominate the western region of the coastal plain. The cryostructures and ice content of this aggregated terrain unit were studied at 26 sites (Fig. 1), and for 21 of them, both the volumetric ice content of soils and wedge-ice volume were estimated (Fig. 6).

High-centered polygons were well developed at all sites (Fig. 7A). They vary in size from 10 to 25 m across. For the western region of the coastal plain, average size of polygons was about 15 m, while for the eastern region the average size was 14 m. Sub-rounded boundaries of central parts of polygons indicate partial thawing of the upper parts of large ice wedges. The maximum width of wedges at some sites reached at least 5 m, while their vertical extent usually did not exceed 4 m.

The ice veins up to 0.2 m wide penetrating into the larger wedges were frequently observed within the modern transient and intermediate layers (Shur, 1988a,b), which divided the active layer from top surfaces of the larger wedges. Such veins have been described in Canadian literature as secondary and tertiary ice wedges (Lewkowicz, 1994; Mackay, 1976; Wolfe et al., 2000). Mackay (2000) in his later work used these terms to describe ice wedges forming as a result of subsequent subdivision of primary polygons. In this work we use these terms in the similar meaning. In the study area, at the sites with large ice wedges, up to three generations of wedges could be observed within the same polygonal systems: large primary wedges more than 2.5 m wide, medium secondary wedges 0.5 to 1.5 m wide, and small tertiary wedges up to 0.2 m wide. Very often the vertical extents of these wedges were almost identical.

The volumetric wedge-ice content (WIC) of the upper permafrost in the western region of the coastal plain varied from 4% to 28%, and in the eastern region WIC varied from 8% to 16%. Average WIC was slightly higher in the western region (14%) compared to the eastern region

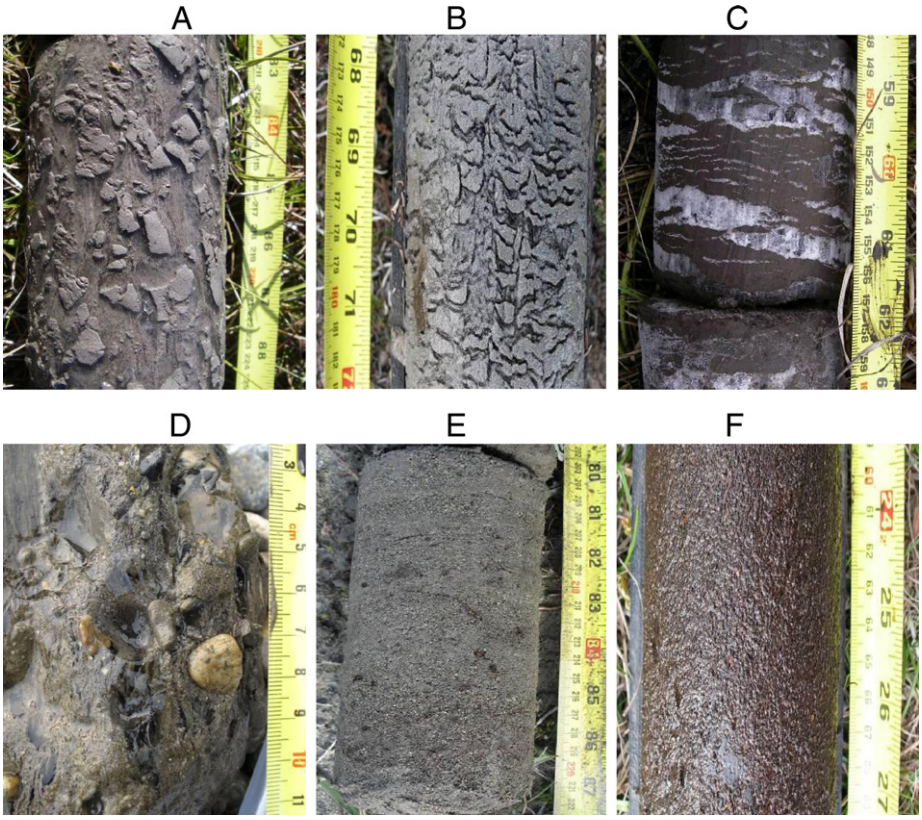

Fig. 4. Dominant cryostructures of the Beaufort Sea Coast. Cryostructures: A — ataxitic (suspended) with angular and sub-angular mineral blocks, site CAHA-E1; B — reticulate with sub-angular mineral blocks, site PBAY-1; C — layered (combined with lenticular and braided), near site BAIS-1; D — crustal (combined with suspended), near site BAIS-1; E — porous, site BSC-45; F — organic-matrix (transitional from organic-matrix suspended to organic-matrix porphyritic), site PBAY-2. For location of sites, see Fig. 1.

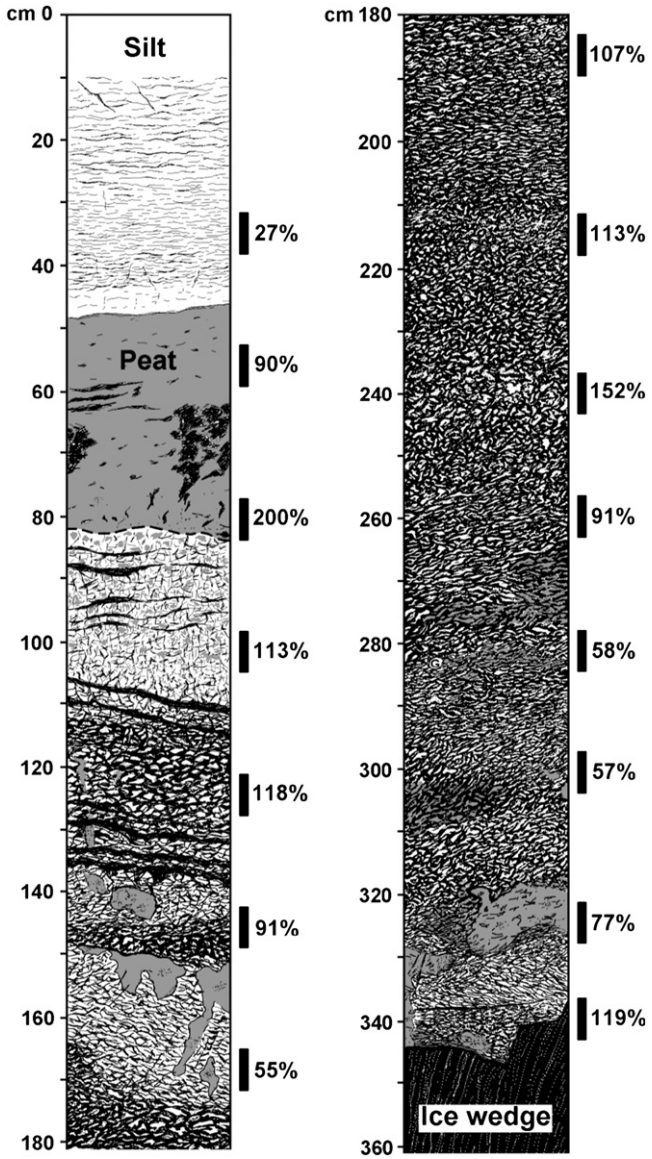

Fig. 5. Cryostratigraphy and gravimetric moisture content of permafrost exposed in the shaft of permafrost tunnel at Barrow, western region of the Arctic Coastal Plain (ice is black). Note the silt deposits with ataxitic cryostructure prevailing in sediments above the buried ice wedge.

(12%). Unusually high WIC was detected in high bluffs in the western region of the coastal plain, where the polygonal network was occasionally very dense with ice wedges of 5 to 7 m apart and up to 5 m in width. Site CAHA-1, located near McLeod Point had the highest wedge-ice volume (28%). The elevation of the bluff there ranged from 5 to 7 m above water level and was the highest for the western region of the coastal plain. Black (1983) at the same site described ice wedges as being 5 to 7 m (max. 9 m) in width. For our calculations of the wedge-ice volume at site CAHA-1, we assumed that the average width of ice wedges was 3 m and the average size of polygons was 10 m. The vertical extent of ice wedges was up to 5 m. In fact the shape of wedges here was not triangular because the width of wedges very often did not decrease significantly with depth, so the wedge-ice volume was underestimated in this case.

Large masses of folded massive ice were identified in a 2-km-long section of coastal bluff near the village of Kaktovik at Barter Island (sites BAIS-1,2,3 in Fig. 1). The exposed ice bodies were as much as 6 to 7 m thick and up to 15 m wide as individual masses and occurred at irregular depths, varying from just below the active layer to a depth of 6 to 8 m (Fig. 8). The ice masses were highly deformed and differently oriented (vertical, horizontal, inclined) and shaped (straight, wavy, folded). The ice was stratified with layers and inclusions of sand and gravel, which were irregularly shaped with numerous folds. We interpret this ice as buried basal glacier ice (Jorgenson and Shur, 2008; Kanevskiy et al., 2008, 2011b). Several years before our observations at Barter Island, Shur et al. (2001) hypothesized that the Arctic Coastal Plain of northern Alaska was glaciated during the Late Pleistocene. They based this hypothesis on the absence of yedoma in most of the arctic coastal region of Alaska, while in comparable arctic regions of Siberia and Alaska, which remained unglaciated during the Late Pleistocene, yedoma occurs widely. Our measurements at the 600-m-long and 7- to 10-m-high coastal exposure showed that the folded massive ice in this section occupied 19% of the face of the bluff, the wedge ice occupied 14%, and the thermokarst-cave ice occupied 2%. Thus, the total area occupied by massive ice was 35% of the face of the bluff (Kanevskiy et al., 2008, 2011b).

Peat was abundant in the active layer, and organic-rich soil was common in the upper permafrost at both the eastern and western regions of the coastal plain. The thickness of organic-rich soil in the upper permafrost reached 130 cm at some sites, with an average of 56 cm in the western region of the coastal plain and 35 cm in the eastern region. The cryostructure of organic soils was predominantly organic-matrix (Figs. 9, 10). Organic soils with an organic-matrix suspended cryostructure were ice-rich and organic soils with the organic-matrix porphyritic cryostructure were relatively ice-poor.

Mineral fine-grained soils (silts, silty sands, and silty clays) of the upper permafrost had mainly ataxitic and reticulate cryostructures (Figs. 9, 10). In studied sections, soil with ataxitic structure occupied 65% of the total thickness of frozen mineral soils in the western region of the coastal plain and 40% in the eastern region. Typically, the thickness of sediments with the ataxitic cryostructure varied from 0.5 to 2 m. Ice lenses and layers up to 30 cm thick were observed in organic and mineral sediments (Fig. 13). Porous cryostructure was typically observed in sands, although occasionally sands were extremely ice-rich. Gravels and gravelly sands usually had a crustal cryostructure.

Volumetric ice content (VIC) of organic and mineral soils between ice wedges of the primary surface varied from 37% to 91% (Fig. 6).

Table 1
Mean ground ice characteristics in the upper permafrost of major terrain units along the Beaufort Sea coast of Alaska.

Terrain units	Number of sites	Thaw depth, cm (end July–mid August)	Portion of frozen soil with ataxitic cryostructure in section, %	Volume of pore and segregated ice in soil, %	Wedge ice		Total ice volume, %
					Size of polygons, m	Wedge-ice volume, %	
1. Primary surface of the coastal plain	26	48	50	80	14	13	83
2. Low foothills (Yedoma)	2	50	80	80	8	50	89
3. Drained-lake basins	19	41	46	81	20	8	82
4. Deltas and tidal flats	12	63	23	72	22	6	73
5. Eolian sand dunes	6	80	0	39	16	4	43

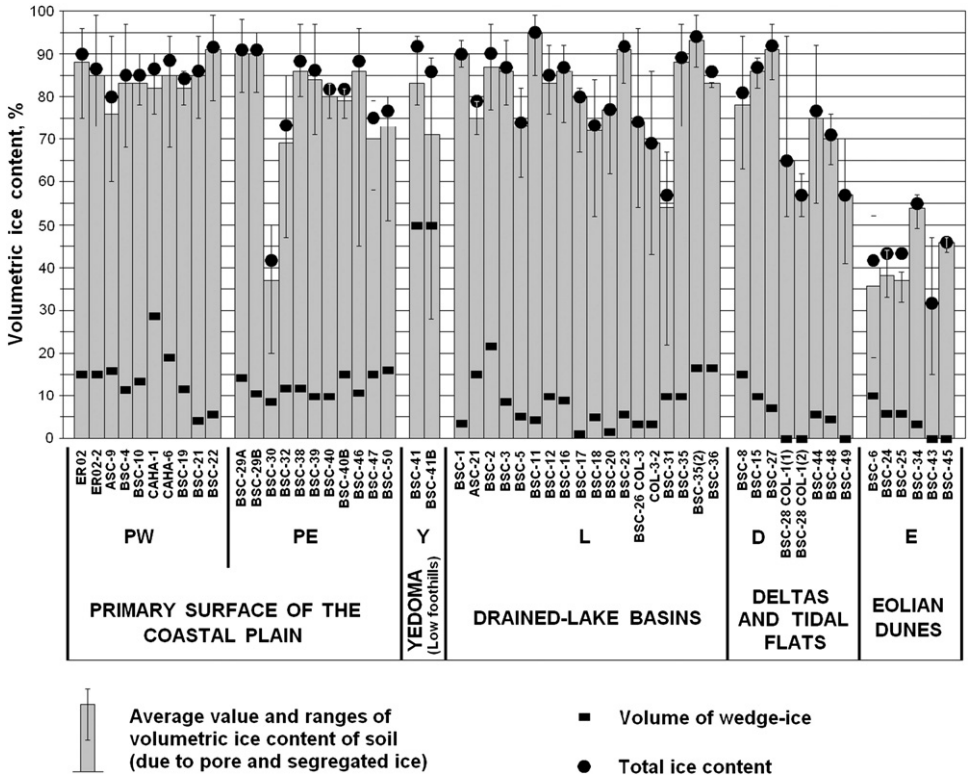

Fig. 6. Volumetric ice content of the upper permafrost. Total volumetric ice content (TVIC) includes wedge ice, segregated ice, and pore ice. PW primary surface of the coastal plain, western region (mostly silty deposits; average TVIC — 86%); PE — primary surface of the coastal plain, eastern region (mostly gravelly deposits; average TVIC — 80%); Y — yedoma (silt; average TVIC — 89%); L — drained — lake basins (mostly silt; average TVIC — 82%); D — deltas and tidal flats (mostly silt and sand; average TVIC — 73%); E — eolian dunes (sand; average TVIC — 43%).

Mineral soils with the ataxitic cryostructure had the highest VIC, reaching 90% and even 95%. The visible ice content of these sediments varied from 50% to 80% (Figs. 4A, 9). Lower ice contents were typically observed only in sand and gravel. The average VIC of soils, including segregated and pore ice (without wedge ice), for all sites reached 84% in the western region of the coastal plain (PW) and 77% in the eastern region (PE). The average total volumetric ice content (TVIC), which includes wedge ice, segregated ice, and pore ice, was 86% in the western region of the coastal plain, and 80% in the eastern region. The average TVIC for the entire primary surface of the Arctic Coastal Plain was 83% (Table 1).

4.2.2. Yedoma of low foothills

Along the BSCA, extremely ice-rich Pleistocene permafrost (yedoma) occurred only in the 20-km segment of the Camden Bay area (field sites BSC-41 and BSC-41b in Fig. 1). Large ice wedges were observed at these sites (Fig. 11), but no polygons were visible on the ground surface, which is typical of yedoma with the undisturbed surface. At a distance of about 1.8 km from the coastal bluff, retrogressive thaw slumps and numerous conical thermokarst mounds (baidzharakhs), typical of yedoma, were evident on satellite images. The size of the polygons at this location varied from 6 to 10 m across; the width of the ice wedges varied from 1 to 4 m. Based on these measurements and observations at field sites BSC-41 and BSC-41b, estimated WIC for these sites was about 50%. Total volumetric ice content including wedge ice, pore ice, and segregated ice was 89% (Fig. 8, Table 1). Yedoma structure and its properties in the Camden Bay area are yet to be studied in more detail.

Yedoma observed at the Camden Bay was similar to the sections described by Carter (1988) in the low foothills of the Brooks Range, where continuous areas of eolian silt (loess) contain large ice wedges. According to Carter, these areas form a belt 5 to 70 km wide at the boundary between the Arctic Coastal Plain and the Arctic Foothills. In the Camden Bay area, eolian silt of Pleistocene age was mapped by Carter et al. (1986). The loess belt contains thick sequences of ice-rich syngenetic permafrost, known in the permafrost literature as yedoma. Permafrost within the loess belt was also described by Lawson (1982, 1983) and Brewer et al. (1993). The best yedoma exposure in Alaska was recently described at the 35 m high vertical cut bank of the Itkillik River (69°34′ N, 150°52′ W) (Kanevskiy et al., 2011a,b).

4.2.3. Drained-lake basins

Drained-lake basins of different ages are numerous in the Arctic Coastal Plain, especially in its western region. Flat polygons and low-centered polygons associated with active ice wedge formation were common in relatively young drained-lake basins, while the polygons of old basins were mostly high-centered. Polygons were predominantly tetra-, penta-, and hexagonal in shape, and had mostly angular shapes (Fig. 7B). Their size varied from 11 to 60 m, with the largest polygons in young basins. The average size of polygons in young (6 sites) and old (13 sites) lake basins was 33 m and 18 m, respectively. The average size of polygons for all 19 sites was 20 m, which was 25% larger than the average size of polygons on the primary surface of the Arctic Coastal Plain. The decrease in sizes of polygons from young to old basins, and then to the oldest primary surface, indicates that polygons are subdivided over time.

Wedge-ice volume in drained-lake basins varied from less than 1% in young basins to 22% in old basins, and averaged WIC was 8%. For young lake basins, average WIC was 3%. Old drained-lake basins had the highest volume of wedge ice (11% average), which was only slightly smaller than values typical of the primary surface of the Arctic Coastal Plain. The process of wedge-ice formation in the artificially drained lake in the Canadian Arctic was studied in details by Mackay (1997) and Mackay and Burn (2002). At that site, the growth of ice wedges was consequent to formation of extremely wide (3 to 20 cm) contraction

cracks occurring in 1978, the first winter after the drainage. After 12 years of intensive cracking and wedge-ice formation, the cessation of cracking occurred due to vegetation growth and increased snow accumulation.

A thickness of layer of organic-rich soil varied from 0 to 20 cm in young drained-lake basins to more than 1 m in some old basins. The average thickness of frozen organic-rich soil in old basins was 47 cm, which was similar to the primary surface of the Arctic Coastal Plain. The most common cryostructure of organic soils was organic-matrix.

Ataxitic, reticulate, layered, and lenticular cryostructures (Figs. 12, 13) are typical of mineral fine-grained soils of the upper permafrost of drained-lake basins. The average fraction of frozen mineral soil with ataxitic cryostructure was 59% for old basins and 33% for young basins with the average for all basins of 46%, which is smaller in comparison with the primary surface of the coastal plain. Occasionally thick, distinct ice layers ("belts") parallel to the surface were found in sediments of drained-lake basins (Figs. 12, 13). VIC between ice wedges (due to segregated and pore ice) varied from 54% to 95% (Fig. 6). The average VIC in drained-lake basins reached 81% and TVIC averages 82%. Generally, the cryogenic structure and ice content of soils of old drained-lake basins are similar to those of the primary surface of the Arctic Coastal Plain (Fig. 6, Table 1).

4.2.4. Deltas and tidal flats

The upper permafrost of deltas and tidal flats was sampled at 12 sites. Ice-wedge polygons were well developed at 9 sites. At 5 sites, a polygonal network had not developed yet. Polygons varied in size from 15 to 35 m, with an average size of 22 m. Greatest sizes of polygons were typical for the active delta, where sedimentation continues (Fig. 7C). These polygons were predominantly low-centered or flat. WIC at deltas and tidal flats varied from 0% to 15% and averaged 6% (Fig. 6, Table 1). The lowest WIC occurred on young surfaces with continuing sediment accumulation. For example, polygons were not observed on a low deltaic surface near the seashore, such as site COL-1 at the Colville River Delta. At inactive delta floodplains, polygons were mostly high-centered, and WIC varied from 7% to 15%.

Thickness of frozen peat and organic-rich soil averaged 23 cm, which was much thinner than on the primary surface of the coastal plain and in old lake basins. The cryostructure of organic soils in deltaic deposits was organic-matrix. Cryostructures in the perennially frozen silty and clayey soils of active channel deposits were predominantly porous and braided. In the inactive delta not affected by recent sediment accumulation, the cryostructure was reticulate and ataxitic. The fraction of frozen mineral soil with ataxitic cryostructure in delta and tidal flats deposits averaged 23%, which was much smaller than in most of the other terrain units (Table 1). Examples of cryogenic structure of deltaic soils at two field sites on the Colville River Delta are shown in Fig. 14.

Average VIC in deltas varied from 57% to 91% (without wedge ice) and averaged 72%. The lowest values (57% to 65%) are typical of soils of young deltas. TVIC averaged 73%. Generally, the ice content of delta and tidal flat deposits is lower in comparison with other terrain units (Table 1).

4.2.5. Eolian sand dunes

Ground ice in eolian sand was studied at six sites. Two sites (BSC-24 and BSC-25) were located within the Late Pleistocene "sand

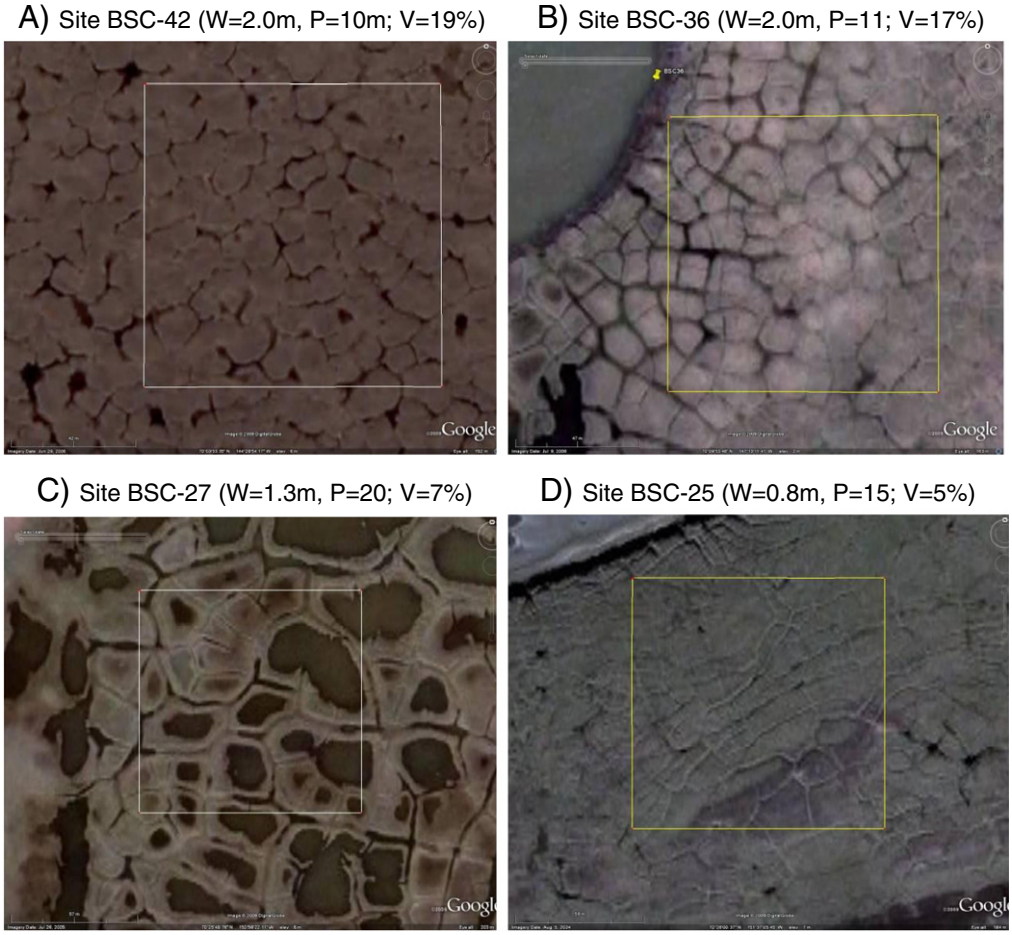

Fig. 7. Ice-wedge polygons typical of various terrain units. A — primary surface of the coastal plain; B — old drained-lake basins; C — deltas; D — stabilized eolian sand dunes. Locations of sites are shown in Fig. 1. Squares are 100×100 m^2 (squares were used for estimation of the polygon size); W — average width of wedges; P — average size of polygons; V — wedge-ice volume.

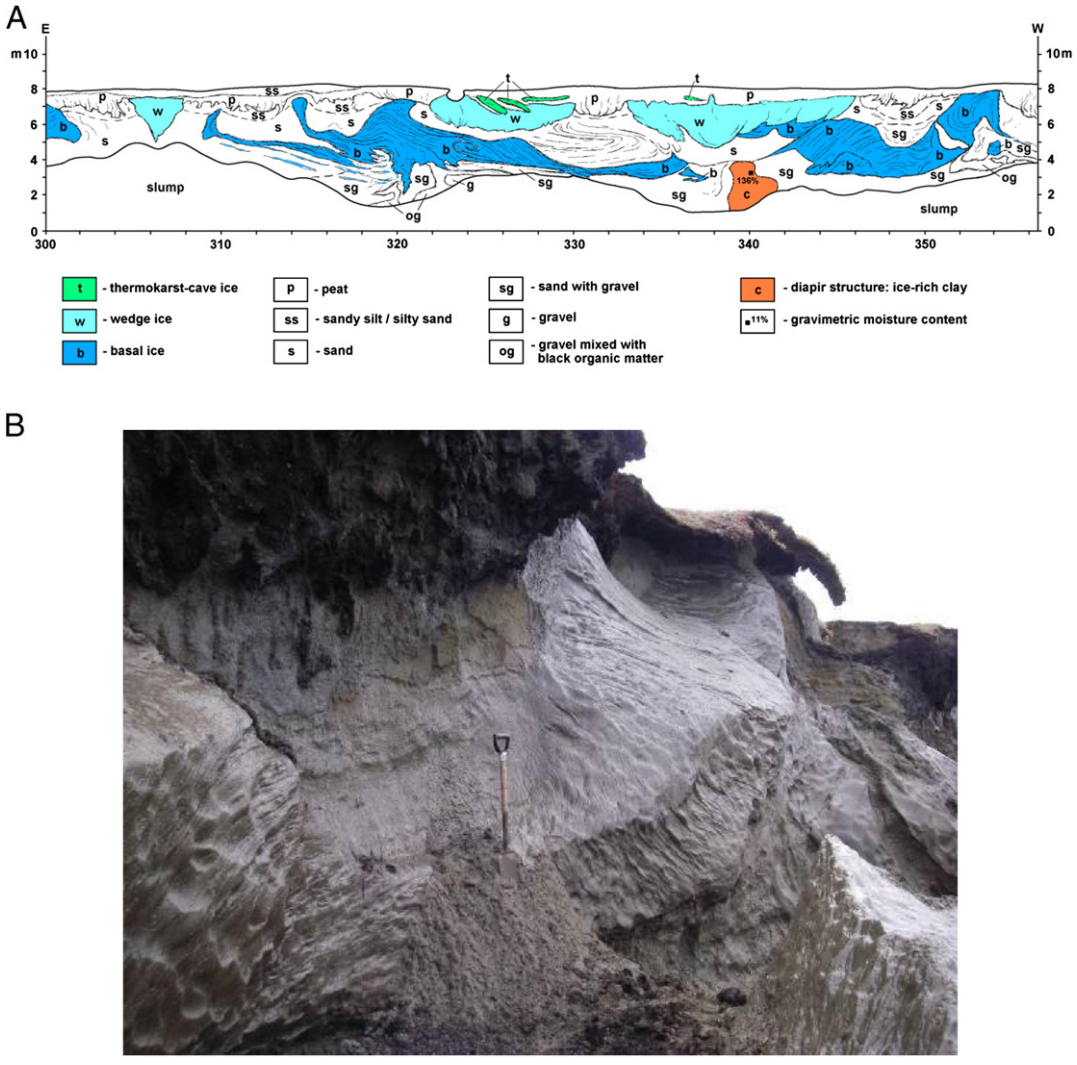

Fig. 8. A — Fragment of cryostratigraphic map of the 600-m-long section KAKT-7, Barter Island (near the sites BAIS-1,2,3; location of sites is shown in Fig. 1), 300–356 m. Radiocarbon ages of two samples taken from organic-rich gravel layers (og) exceed 48,000 ^{14}C yr BP. B — Folded massive ice body, section KAKT-7, 280–298 m.

sea" (Carter, 1981) with stabilized eolian dunes. Four other sites with modern sand dunes were located in deltaic areas.

Unlike other terrain units, organic horizons on sand dunes were very poorly developed. Thin surficial peat layer was observed at one site only. No frozen organic-rich soils were detected. Small buried sand wedges up to 0.6 m wide with vertical extent up to 1 m were described in the section of eolian sand in the vicinity of site BSC-22(PW). Sand wedges up to 3 m wide and up to 7 m deep had been described in this area by Carter (1983b), who related their formation to extremely cold arid conditions of the Late Pleistocene.

Ice-wedge polygons were found at four sites with vegetated eolian dunes. Average size of polygons for these sites varied from 13 to 21 m and averaged 16 m. Many polygons had elongated shape (Fig. 7D). No ice wedges were exposed at these study sites, and the width of ice wedges was estimated through the width of troughs over degrading wedges. In most cases, the estimated width of ice wedges did not exceed 1 m. Average WIC for these sites was 6%. No wedges were detected at sites BSC-43 and BSC-45 where active sand dunes had no vegetation. Average WIC for eolian dunes was 4%.

Eolian sand has mostly porous cryostructure without visible excess ice. Volumetric ice content of eolian sand averaged 41%. For different field sites the average volumetric ice content varied from 32% to 54%, which is in a range of porosity of unfrozen sands. Total ice volume, which includes wedge ice, segregated ice and pore ice averaged 43%, which is the lowest for all studied terrain units on the Arctic Coastal Plain. The low ice content and lack of segregated ice can be explained by low frost susceptibility of sands and low moisture content in the active layer formed by well drained eolian sands.

4.3. Development of the intermediate layer in upper permafrost

One of the most striking permafrost features is the prevalence of the horizon of very ice-rich soil in the upper permafrost, which Shur (1988a,b) has termed the *intermediate layer*. The main diagnostic characteristic of the intermediate layer is its ataxitic cryostructure. This cryostructure is abundant in most of the terrain units of the BSCA (Table 1).

The intermediate layer forms as a result of gradual decrease in the active layer thickness after termination of sedimentation (Shur, 1988a,b), under the impact of vegetation succession, changes of surface conditions, and other various local factors (Lewkowicz, 1994; Mackay, 1997; Shur, 1988a,b). The intermediate layer is formed by the upward permafrost aggradation due to accumulation of an organic horizon on the soil surface whose insulating properties increase with time (Ping et al., 2008a; Shur, 1988a,b; Shur and Ping, 1993). With the accumulation of organic matter above the mineral soil, some part of the initial active layer or its entire mineral part joins the permafrost. Because this process is very slow and continuing over centuries, the upper permafrost layer is

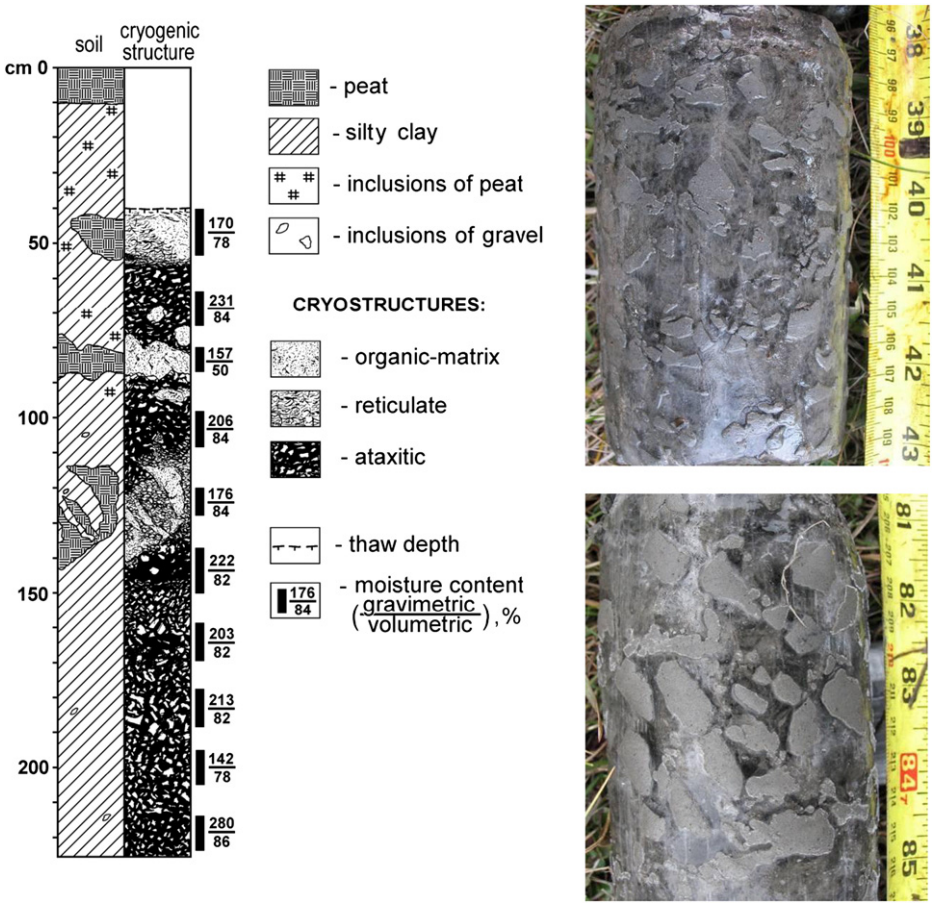

Fig. 9. Cryostratigraphy of deposits of the primary surface of the coastal plain, field site BSC-19. Height of the bluff is 2.7 m. Location of site is shown in Fig. 1. Photographs show the details of ataxitic (suspended) cryostructure, prevailing at this site. Radiocarbon dates: 45–47 cm — 2700 ± 30 ^{14}C yr BP; 140–142 cm — 9370 ± 50 ^{14}C yr BP.

extremely ice-rich and has a distinctive ataxitic cryostructure. During the formation of the intermediate layer, the surface rises gradually as a result of perennial frost heave due to accumulation of excess aggradational ice (Mackay, 1972) in this layer. Thus formation of these ice-rich deposits is a very important factor in the elevation of the generally low surface of the Beaufort Coastal Plain.

Increase in thickness of the ice-rich layer formed from the initial active layer can be evaluated with the following equations (Fig. 15):

$$\Delta = \frac{b-a}{a} \tag{3}$$

and

$$b = a + \Delta a = a(1+\Delta), \tag{4}$$

where

a thickness of the part of active layer, transforming into permafrost,
b thickness of the intermediate layer,
Δ freezing swell of soil due to accumulation of the aggradational ice (including pore and segregated ice).

Δ can be found knowing void ratio (e) or porosity (n) of soil in the intermediate layer and soil in the initial active layer:

$$\Delta = \frac{e_2-e_1}{1+e_1}, \tag{5}$$

or

$$\Delta = \frac{n_2-n_1}{1+n_1}, \tag{6}$$

where

e_1 and n_1 void ratio and porosity of soil of the active layer prior aggradational ice accumulation,
e_2 and n_2 void ratio and porosity of the intermediate layer after aggradational ice accumulation.

The average volumetric ice content (porosity) of silty soils with ataxitic cryostructure in the Arctic Coastal Plain is about 80%, or 0.8 measured as a fraction of a unit. An average porosity of unfrozen soil prior to aggradational ice formation can be conservatively assumed as 0.5. Consequently, $\Delta \cong 1.5$ and $b = 2.5a$. If a thickness of the part of the active layer, transforming into permafrost, was between 0.3 and 0.5 m, the thickness of the intermediate layer can reach 0.75 to 1.25 m, which is in agreement with numerous field data on the intermediate layer (Shur, 1988a,b).

A comparison of cryogenic structure and ice content in soils of the main terrain units (except sand dunes) shows that accumulation of aggradational ice in the upper permafrost is typical of the old terrain units and practically does not depend on their genesis. The ataxitic cryostructure (the main diagnostic characteristic of the intermediate layer) is abundant in the terrain units of the primary surface of the coastal plain; it is also common in older stages of drained-lake basins

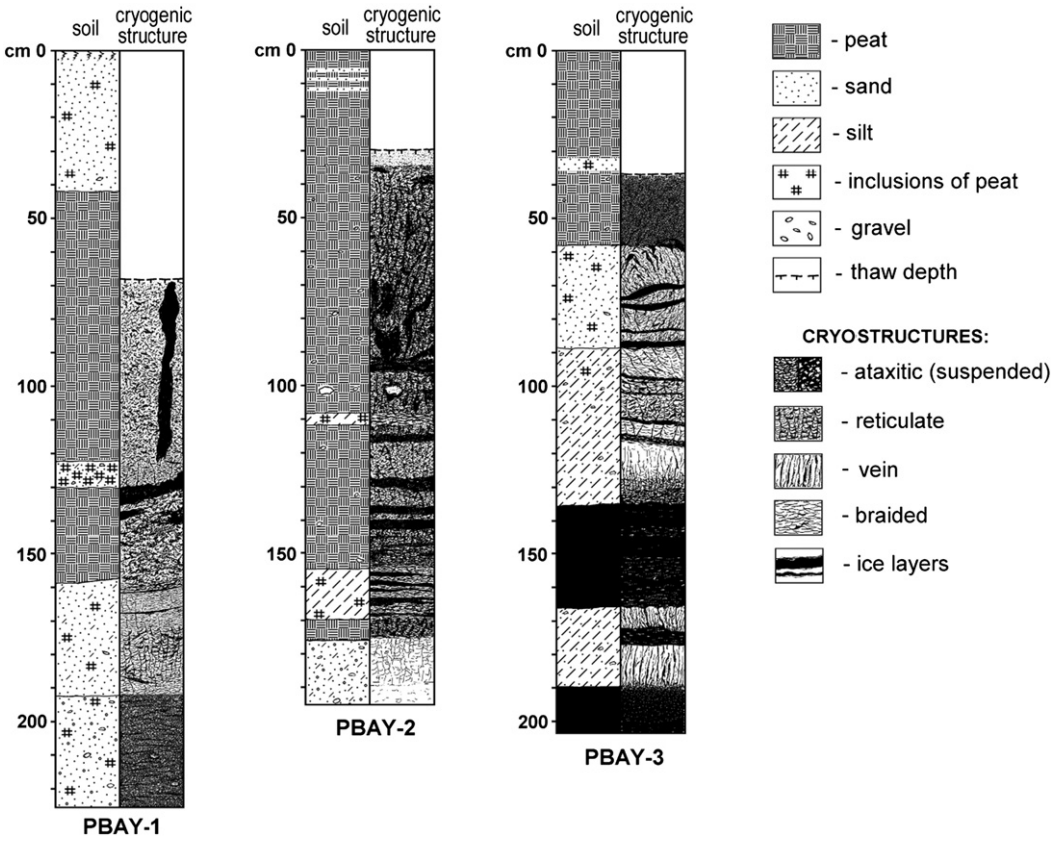

Fig. 10. Cryostratigraphy of deposits of the primary surface of the coastal plain, field sites PBAY-1 (height of the bluff is 2.5 m), PBAY-2 (height of the bluff is 1.5 m), and PBAY-3 (height of the bluff is 2 m). Location of sites is shown in Fig. 1. Radiocarbon date: 8950 ± 40 ^{14}C yr BP (site PBAY-1, depth 160–170 cm).

and deltas where ground ice volumes are similar to those of the primary surface.

The majority of samples of the basal peat (obtained from the boundary between organic-rich soil and mineral soil) from such different terrain units as primary surface of the coastal plain, low foothills, and drained-lake basins had approximately the same age: mostly from 6000 to 10,000 ^{14}C yr BP, and it did not depend on the thickness of peat (several radiocarbon dates are shown in Figs. 9, 10, 13, and 14). It means that accumulation of peat (and consequent formation of the intermediate layer) started almost simultaneously at terrain units which were not affected by thermokarst (primary surface of the coastal plain and low foothills) and at the oldest drained-lake basins.

An intermediate layer in most cases was not detected in recently drained lake basins and modern deltas, where accumulation of

Fig. 11. Yedoma silt with large ice wedges, site BSC-41.

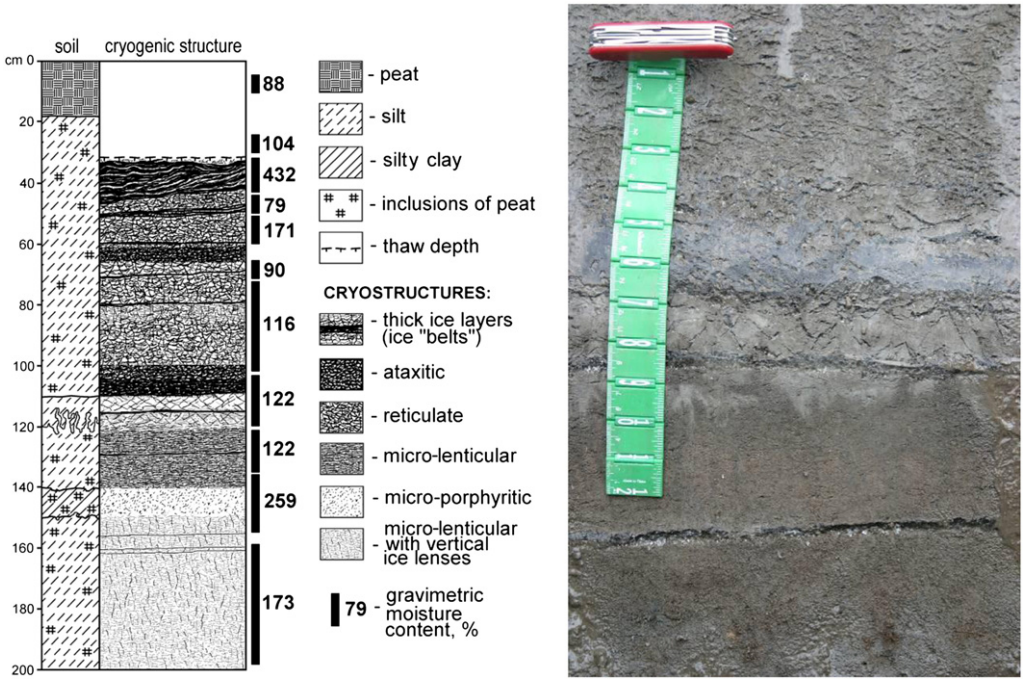

Fig. 12. Cryostratigraphy of drained-lake basin deposits, coastal exposure at the field site ASC-21 (height of the bluff is 2.3 m). Location of site is shown in Fig. 1. Photograph shows the details of cryogenic structure, depth 90–140 cm.

organic matter has not started yet. Initial stage of the intermediate layer formation was observed at the field site COL-1 located on poorly vegetated tidal flats. While the section of borehole COL 1-2 contained no visible ice (porous invisible cryostructure), the 90 cm thick layer right below the permafrost table in borehole COL 1-1 was mostly ice-rich (Fig. 14). We attribute this to formation of the intermediate layer as a result of a decrease in the active layer thickness from 115 to 55 cm due to accumulation of organic matter. Borehole COL 2-1

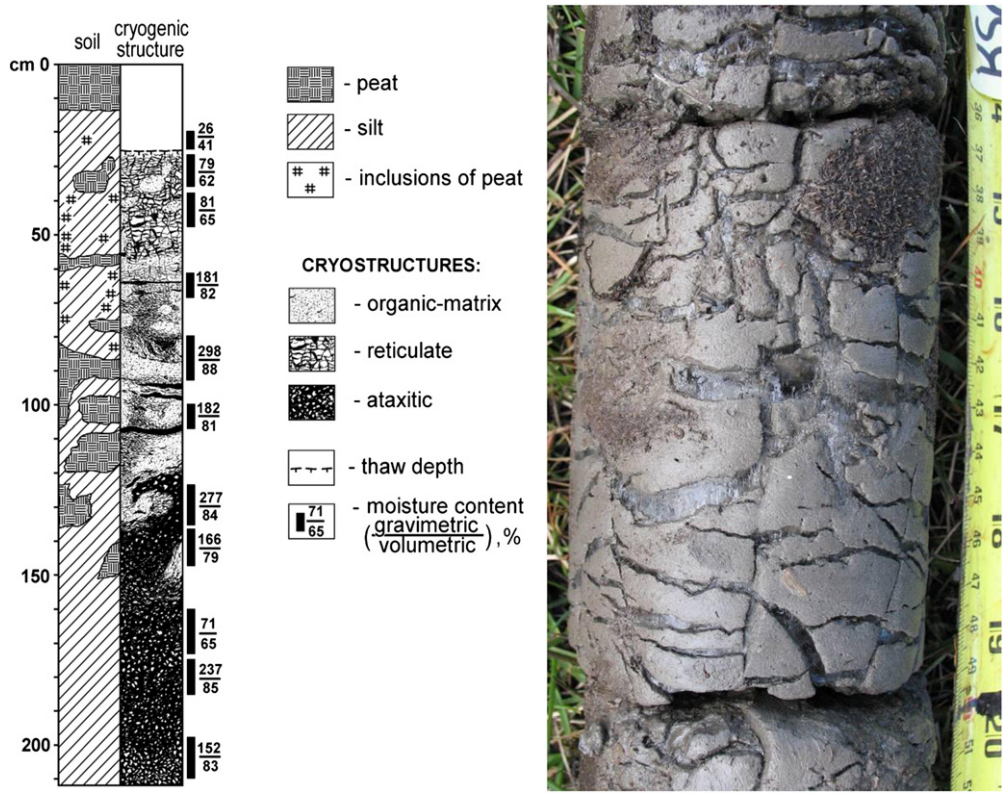

Fig. 13. Cryostratigraphy of drained-lake basin deposits, field site BSC-20 (height of the bluff is 2.5 m). Location of site is shown in Fig. 1. Photograph shows the details of reticulate cryostructure of silt. Radiocarbon dates: 315 ± 25 ^{14}C yr BP (depth 23–25 cm); 8160 ± 45 ^{14}C yr BP (depth 155–158 cm).

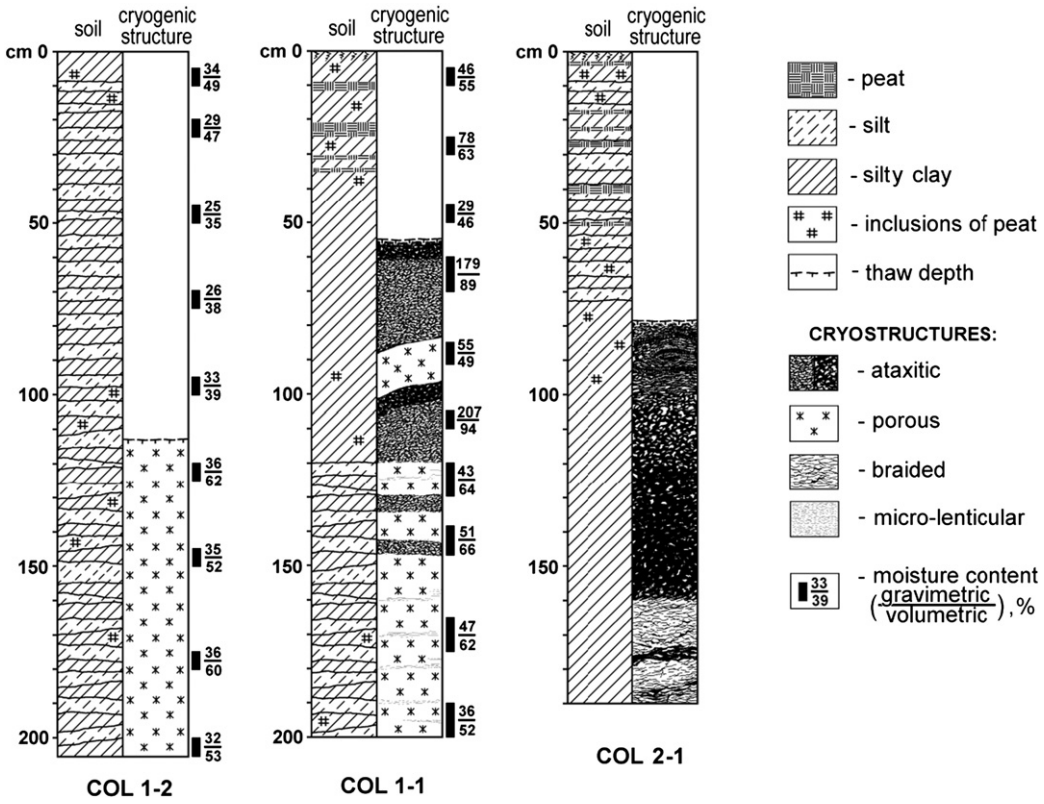

Fig. 14. Cryostratigraphy of deltaic deposits, Colville River Delta, field sites COL-1 (0.2 m above the sea level), COL-2 (height of the bluff is 1 m). Location of sites is shown in Fig. 1. Radiocarbon dates: 4820±40 ^{14}C yr BP (site COL1-2, depth 100–101 cm); 2500±35 ^{14}C yr BP (site COL1-2, depth 115–116 cm); 1550±35 ^{14}C yr BP (site COL1-1, depth 35–36 cm); 3310±40 14C yr BP (site COL2-1, depth 55–57 cm).

was located more than 900 m from boreholes COL 1-1 and COL 1-2 at the 0.8- to 1.0-m-high bank of the active delta channel. Sediments here had a mostly ataxitic cryostructure and were extremely ice-rich.

No intermediate layer was observed in the eolian sand dunes, even within the Late Pleistocene "Sand Sea". It can be explained by the absence of organic layer on the soil surface, whose accumulation leads to decrease in the active layer thickness and formation of the intermediate layer, and by the low frost susceptibility of sands as well.

There is a close correlation between the occurrence of the ice-rich layer with ataxitic cryostructure and thickness of the active layer in different terrain units. At the primary surface of the coastal plain and drained-lake basins, for which ataxitic cryostructure was the most common (Table 1), the average thaw depth measured from the end of July till the middle of August was 41 and 48 cm correspondingly, and at some sites it did not exceed 30 cm. At deltas and tidal flats, where the average occurrence of ataxitic cryostructure was 23%, the average thaw depth was 63 cm. At the poorly vegetated eolian sand dunes, the average thaw depth reached 80 cm, and no ice-rich sediments were detected.

Occurrence of the ice-rich layer of the upper permafrost in the adjacent areas of Canadian Arctic has been explained by decrease in the active layer thickness after its dramatic increase during the Holocene climatic optimum (Burn, 1997; Mackay, 1978; Pollard, 1990). Our studies (Jorgenson et al., 1998; Shur, 1988a,b; Shur and Jorgenson, 1998) show that contemporary formation of the intermediate layer is a result of decrease in the active layer thickness, which takes place with organic accumulation on the soil surface and is not necessarily related to climate changes.

5. Conclusions

The types and volume of ground ice across the BSCA were variable depending on types of terrain units and associated soil texture, and the age of the material, which affects the development of the intermediate layer and ice wedges over time. Most of the BSCA soils are frost-susceptible silty soils, and therefore most of the upper permafrost was extremely ice-rich and dominated by ataxitic cryostructure.

The ice content of the upper permafrost of most of the main terrain units with silty soils is practically the same. Terrain units with recent sediment deposition without vegetation had thicker active layers. Ice wedges in such terrain units were at the initial stage of development or absent. The ice content of the upper permafrost there was low, the intermediate layer was undeveloped, and ataxitic cryostructure was absent. With the accumulation of organic matter, the depth of the active

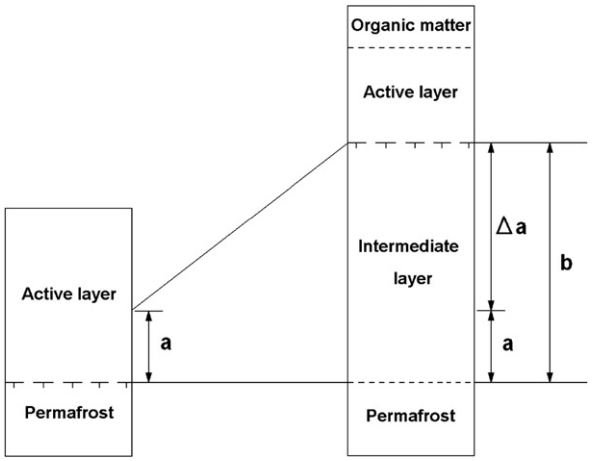

Fig. 15. Formation of the intermediate layer of upper permafrost. a = thickness of the lower part of active layer transforming into permafrost; b = thickness of the intermediate layer; Δ = freezing swell of soil due to aggradational ice formation.

layer decreased, leading to formation of the intermediate layer with ataxitic cryostructure and accumulation of aggradational ice.

The ice content (first of all, wedge-ice content) is notably lower in young drained-lake basins, deltas, and tidal flats than in older terrain units associated with the primary surface of the coastal plain, mature drained-lake basins, and inactive deltas. We attribute this difference to modification of the upper permafrost with time related to vegetation and soil development. The older the sites in drained-lake basins and deltas with their silty soils, the more similar the cryogenic structure and the total ice content of upper permafrost become to those of the primary surface, due to the accumulation of organic matter and the development of the intermediate layer of the upper permafrost. In contrast, eolian sand dunes with their sandy soils greatly reduce the potential for segregated ice formation and development of thick intermediate layers, and for formation of thick ice wedges as well.

Average volumetric wedge-ice content (WIC) varied widely between terrain units, ranging from 3% to 50%. The highest WIC reached more than 50% in yedoma of the Lower Foothills. For the old primary surfaces of the Arctic Coastal Plain, average WIC was similar between the western (14%) and eastern (12%) regions. Old drained-lake basins (11%) had much higher wedge-ice volume than young basins (3%). Average WIC on young delta deposits (3%) and modern eolian sand dunes (3%) also were low. For the majority of sites, except areas with young and old eolian sand dunes, young deltas, and young drained-lake basins, average values of total volumetric ice content (due to wedge, segregated, and pore ice) ranged from 80% to 90%. The lowest value was detected in eolian sand dunes (43%). The total average volumetric ice content for the whole BSCA was 77%.

Accumulation of organic matter and aggradational ice is the result of a combination of factors including cold climate, flat relief, poor drainage, predominantly fine grained soils, and time. Perennial frost heave along with peat accumulation elevates the surface in 1 to 3 m. This is a significant increase for low-lying areas of the Arctic Coastal Plain. Except for the sand dunes and sandy and gravelly floodplains, the occurrence of the ice-rich intermediate layer of the upper permafrost is a widespread and important characteristic of the Arctic Coastal Plain.

Acknowledgments

This study was supported by the National Science Foundation grants OPP-0436179, ARC-0436165, ARC-0454985, and ARC-0454939, and Alaska EPSCoR, funded by the NSF grant 0701898 and the State of Alaska. We would like to thank the Fairbanks office of Polar Field Services, Inc. (part of CH2M Hill Polar Services), the Barrow Arctic Science Consortium, David Payer with U.S. Fish and Wildlife Service, Troy Cambier, helicopter pilot, and James and Teena Helmericks for their logistical support. Dorte Dissing, ABR, provided GIS services. Prothap Kodeal, Fugen Dou, and Lorene Lynn participated in sampling at field sites.

We would like to thank Fran Pedersen, UAF, and two anonymous reviewers for valuable comments and suggestions.

References

Black, R.F., 1952. Growth of ice-wedge polygons in permafrost near Barrow, Alaska. Bulletin of the Geological Society of America 63, 1235–1236.

Black, R.F., 1964. Gubik Formation of Quaternary age in northern Alaska. U.S. Geological Survey Professional Paper 302-C, pp. 59–91.

Black, R.F., 1983. Three superimposed systems of ice wedges at McLeod Point, northern Alaska, may span most of Wisconsinan stage and Holocene. Permafrost: Fourth International Conference Proceedings. National Academy Press, Washington, DC, pp. 68–73.

Brewer, M.C., Carter, L.D., Glenn, R., 1993. Sudden drainage of a thaw lake on the Alaskan Arctic Coastal Plain. Proceedings of the Sixth International Conference on Permafrost, July 5–9, Beijing, China. South China University of Technology Press, pp. 48–53.

Brigham, J.K., 1985. Marine stratigraphy and amino-acid geochronology of the Gubik Formation, western Arctic Coastal Plain, Alaska. U.S. Geological Survey Open-File Report 85-381, 218 pp.

Brigham-Grette, J.K., Carter, L.D., 1992. Pliocene marine transgressions of Northern Alaska: circumarctic correlations and paleoclimatic interpretations. Arctic 45 (1), 74–89.

Brown, J., 1965. Radiocarbon dating, Barrow, Alaska. Arctic 18 (1), 36–48.

Brown, J., 1967. Tundra soils formed over ice wedges, northern Alaska. Proceedings — Soil Science Society of America 31 (5), 686–691.

Brown, J., 1969. Ionic concentration gradients in permafrost, Barrow, Alaska. CRREL Research Report 272. Cold Regions Research and Engineering Laboratory, Hanover, NH, 26 pp.

Brown, J., Romanovsky, V.E., 2008. Report from the International Permafrost Association: state of permafrost in the first decade of the 21st century. Permafrost and Periglacial Processes 19 (2), 255–260.

Brown, J., Sellmann, P.V., 1973. Permafrost and coastal plain history of arctic Alaska. In: Britton, M.E. (Ed.), Alaskan Arctic tundra. Technical Paper No. 25. Arctic Institute of North America, pp. 31–47.

Burgess, M.M., Smith, S.L., 2003. 17 years of thaw penetration and surface settlement observations in permafrost terrain along the Norman Wells pipeline, Northwest Territories, Canada. Proceedings of the Eight International Conference on Permafrost. A.A. Balkema Publishers, Lisse, Netherlands, pp. 107–112.

Burn, C.R., 1997. Cryostratigraphy, paleogeography, and climate change during the early Holocene warm interval, western Arctic coast, Canada. Canadian Journal of Earth Sciences 34, 912–925.

Burn, C.R., Zhang, Y., 2009. Permafrost and climate change at Herschel Island (Qikiqtaruq), Yukon Territory, Canada. Journal of Geophysical Research 114, F02001 http://dx.doi.org/10.1029/2008JF001087.

Carter, L.D., 1981. A Pleistocene sand sea on the Alaskan Arctic Coastal Plain. Science 211, 381–383.

Carter, L.D., 1983a. Fossil sand wedges on the Alaskan Arctic Coastal Plain and their paleoenvironmental significance. Permafrost: Fourth International Conference Proceedings. National Academy Press, Washington, DC, pp. 109–114.

Carter, L.D., 1983a. Engineering-geologic maps of northern Alaska, Teshakpuk quadrangle. U.S. Geological Survey Open-File Report 83-634.

Carter, L.D., 1988. Loess and deep thermokarst basins in Arctic Alaska. Proceedings of the Fifth International Conference on Permafrost. Tapir Publishers, Trondheim, Norway, pp. 706–711.

Carter, L.D., Galloway, J.P., 1979. Arctic Coastal Plain pingos in National Petroleum Reserve in Alaska. In: Johnson, K.M., Williams, J.R. (Eds.), U.S. Geological Survey in Alaska; accomplishments during 1978: USGS Circular 804-B, pp. B33–B35.

Carter, L.D., Galloway, J.P., 1985. Engineering-geologic maps of northern Alaska, Harrison Bay quadrangle. U.S. Geological Survey Open-File Report 85-256.

Carter, L.D., Ferrians, O.J., Galloway, J.P., 1986. Engineering-geologic maps of northern Alaska, coastal plain and foothills of the Arctic National Wildlife Refuge. U.S. Geological Survey Open-File Report 86-334, 2 sheets.

Dinter, D.A., Carter, L.D., Brigham-Grette, J.K., 1987. Late Cenozoic geologic evolution of the Alaskan North Slope and adjacent continental shelves. In: Grantz, A., Johnson, L., Sweeney, J.E. (Eds.), The geology of the Arctic Ocean region: Boulder, Colorado, Geological Society, Geology of North America, American Geology, vol. L, pp. 459–490.

Ferrians, O.J., 1988. Pingos in Alaska: a review. Permafrost: Fifth International Conference Proceedings. Tapir Publishers, Trondheim, Norway, pp. 734–739.

French, H.M., 1998. An appraisal of cryostratigraphy in North–West Arctic Canada. Permafrost and Periglacial Processes 9, 297–312.

Gasanov, S.S., 1963. Morphogeneticheskaya klassifikatsia kriogennykh tekstur rykhlykh otlozheniy (Morphogenetic classification of cryostructures of frozen sediments). Trudy SVKNII, vol. 3, Magadan (in Russian).

Grechishchev, S.E., Shur, Y. (Eds.), 1990. Metodicheskie rekomendatsii po uchyotu sostava I strukturno-teksturnogo stroeniya myorzlykh porod pri prognoze razvitiya kriogennykh fiziko-geologicheskikh protsessov. (Implementation of composition and structure of frozen ground in prediction of permafrost related geological hazards (Manual)). Ministry of Geology of USSR, Moscow, 79 pp. (in Russian).

Gryc, G., Patton Jr., W.W., Payne, T.G., 1951. Present Cretaceous stratigraphic nomenclature of northern Alaska. Washington Academy of Sciences Journal 41, 159–167.

Harry, D.G., French, H.M., Pollard, W.H., 1988. Massive ground ice and ice-cored terrain near Sabine Point, Yukon Coastal Plain. Canadian Journal of Earth Sciences 25, 1846–1856.

Hopkins, D.M., 1967. Quaternary marine transgressions in Alaska. The Bering Land Bridge. Stanford University Press, Palo Alto, California, pp. 41–90.

Hussey, K.M., Michelson, R.W., 1966. Tundra relief features near Point Barrow, Alaska. Arctic 19 (2), 162–184.

Jones, B.M., Arp, C.D., Jorgenson, M.T., Hinkel, K.M., Schmutz, J.A., Flint, P.L., 2009. Increase in the rate and uniformity of coastline erosion in Arctic Alaska. Geophysical Research Letters 36, L03503 http://dx.doi.org/10.1029/2008GL036205.

Jones, B.M., Grosse, G., Hinkel, K.M., Arp, C.D., Beck, R.A., Galloway, J.P., Walker, S., 2012. Assessment of pingo distribution and morphometry using an IfSAR derived digital surface model, western Arctic Coastal Plain, Northern Alaska. Geomorphology 138, 1–14.

Jorgenson, M.T., 2011. Coastal region of northern Alaska, Guidebook to permafrost and related features: Alaska Division of Geological & Geophysical Surveys Guidebook 10, 188 p.

Jorgenson, M.T., Brown, J., 2005. Classification of the Alaskan Beaufort Sea Coast and estimation of carbon and sediment inputs from coastal erosion. Geo-Marine Letters 25, 69–80.

Jorgenson, M.T., Shur, Y., 2007. Evolution of lakes and basins in northern Alaska and discussion of the thaw lake cycle. Journal of Geophysical Research 112, F02S17 http://dx.doi.org/10.1029/2006JF000531.

Jorgenson, M.T., Shur, Y., 2008. Glaciation of the coastal plain of Northern Alaska. Eos Transactions, American Geophysical Union 89 (53) Fall Meet. Suppl., Abstract C11D-0544.

Jorgenson, M.T., Shur, Y., Walker, H.J., 1998. Evolution of a permafrost-dominated landscape on the Colville River Delta, northern Alaska. Proceedings of the Seventh International Conference on Permafrost. Yellowknife, Canada, pp. 523–529.

Jorgenson, M.T., Macander, M., Jorgenson, J.C., Ping, C.-L., Harden, J., 2003. Ground ice and carbon characteristics of eroding coastal permafrost at Beaufort Lagoon,

northern Alaska. Proceedings of the Eight International Conference on Permafrost. A.A. Balkema Publishers, Lisse, Netherlands, pp. 495–500.
Jorgenson, T., Yoshikawa, K., Kanevskiy, M., Shur, Y., Romanovsky, V., Marchenko, S., Grosse, G., Brown, J., Jones, B., 2008. Permafrost characteristics of Alaska. In: Kane, D.L., Hinkel, K.M. (Eds.), Proceedings of the Ninth International Conference on Permafrost, Extended Abstracts. June 29–July 3, 2008, Fairbanks, Alaska. Institute of Northern Engineering, University of Alaska Fairbanks, pp. 121–122.
Kanevskiy, M., Jorgenson, T., Shur, Y., Dillon, M., 2008. Buried glacial basal ice along the Beaufort Sea Coast, Northern Alaska. Eos Transactions, American Geophysical Union 89 (53) Fall Meet. Suppl., Abstract C11D-0531.
Kanevskiy, M., Shur, Y., Fortier, D., Jorgenson, M.T., Stephani, E., 2011a. Cryostratigraphy of late Pleistocene syngenetic permafrost (yedoma) in northern Alaska, Itkillik River exposure. Quaternary Research 75, 584–596 http://dx.doi.org/10.1016/j.yqres.2010. 12.003.
Kanevskiy, M., Shur, Y., Jorgenson, M.T., Ping, C.-L., Fortier, D., Stephani, E., Dillon, M., 2011b. Permafrost of Northern Alaska. Proceedings of the Twenty-first International Offshore and Polar Engineering Conference Maui, Hawaii, USA, June 19–24, 2011, pp. 1179–1186. ISBN 978-1-880653-96-8 (Set); ISSN 1098-6189 (Set); www.isope.org.
Kanevskiy, M., Shur, Y., Connor, B., Dillon, M., Stephani, E., O'Donnell, J., 2012. Study of the ice-rich syngenetic permafrost for road design (Interior Alaska). In: Hinkel, K.M. (Ed.), Proceedings of the Tenth International Conference on Permafrost, June 25–29, 2012, Salekhard, Russia. International Contributions, vol. 1. The Northern Publisher, Salekhard, Russia, pp. 191–196.
Katasonov, E.M., 1969. Composition and cryogenic structure of permafrost. Technical Translation 1358. National Research Council of Canada, Ottawa, pp. 25–36.
Kokelj, S.V., Burn, C.R., 2005. Near-surface ground ice in sediments of the Mackenzie Delta, Northwest Territories, Canada. Permafrost and Periglacial Processes 16, 291–303.
Kokelj, S.V., Smith, C.A.S., Burn, C.R., 2002. Physical and chemical characteristics of the active layer and permafrost, Herschel Island, Western Arctic Coast, Canada. Permafrost and Periglacial Processes 13, 171–185.
Lachenbruch, A.H., Sass, J.H., Lawver, L.A., Brewer, M.C., Marshall, B.V., Munroe, R.J., Kennelly Jr., J.P., Galanis Jr., S.P., Moses Jr., T.H., 1988. Temperature and depth of permafrost on the Arctic slope of Alaska. In: Gryc, G. (Ed.), Geology and exploration of the National Petroleum Reserve in Alaska, 1974 to 1982: U.S. Geological Survey Professional Paper 1399, pp. 645–656.
Lawson, D.E., 1982. Long-term modifications of perennially frozen sediment and terrain at East Oumalik, northern Alaska. CRREL Report 82-36, 33 pp.
Lawson, D.E., 1983. Ground ice in perennially frozen sediments, northern Alaska. Permafrost: Fourth International Conference Proceedings. National Academy Press, Washington, DC, pp. 695–700.
Leffingwell, E. de K., 1915. Ground-ice wedges, the dominant form of ground-ice on the north coast of Alaska. Journal of Geology 23, 635–654.
Leffingwell, E. de K., 1919. The Canning River region, northern Alaska. U.S. Geological Survey Professional Paper 109, 251 pp.
Lewkowicz, A.G., 1994. Ice-wedge rejuvenation, Fosheim Peninsula, Ellesmere Island, Canada. Permafrost and Periglacial Processes 5, 251–268.
Mackay, J.R., 1972. The world of underground ice. Annals of the Association of American Geographers 62 (1), 1–22.
Mackay, J.R., 1976. Ice wedges as indicators of recent climatic change, Western Arctic coast. Current Research, Part A, Geological Survey of Canada Paper, 76-1A, pp. 523–524.
Mackay, J.R., 1978. Freshwater shelled invertebrate indicators of paleoclimate in northwestern Canada during late glacial times: discussion. Canadian Journal of Earth Sciences 15, 461–462.
Mackay, J.R., 1997. A full-scale field experiment (1978–1995) on the growth of permafrost by means of lake drainage, western Arctic coast: a discussion of the method and some results. Canadian Journal of Earth Sciences 34, 17–33.
Mackay, J.R., 2000. Thermally induced movements in ice-wedge polygons, western Arctic coast: a long-term study. Geographie Physique et Quaternaire 54 (1), 41–68.
Mackay, J.R., Burn, C.R., 2002. The first 20 years (1978–1979 to 1998–1999) of ice-wedge growth at the Illisarvik experimental drained lake site, western Arctic coast, Canada. Canadian Journal of Earth Science 39, 95–111.
Mackay, J.R., Dallimore, S.R., 1992. Massive ice of the Tuktoyaktuk area, western Arctic coast, Canada. Canadian Journal of Earth Sciences 29, 1235–1249.
Melnikov, V.P., Spesivtsev, V.I., 2000. Cryogenic Formations in the Earth's Lithosphere (Graphic Version). Siberian Publishing Center UIGGM, Siberian Branch of the RAS Publishing House, Novosibirsk, 343 pp.
Meyer, H., Schirrmeister, L., Andreev, A., Wagner, D., Hubberten, H.-W., Yoshikawa, K., Bobrov, A., Wetterich, S., Opel, T., Kandiano, E., Brown, J., 2010. Lateglacial and Holocene isotopic and environmental history of northern coastal Alaska — results from a buried ice-wedge system at Barrow. Quaternary Science Reviews 29, 3720–3735.
Morse, P.D., Burn, C.R., Kokelj, S.V., 2009. Near-surface ground-ice distribution, Kendall Island Bird Sanctuary, Western Arctic Coast, Canada. Permafrost and Periglacial Processes 20, 155–171.
Murton, J.B., 2005. Ground-ice stratigraphy and formation at North Head, Tuktoyaktuk Coastlands, western Arctic Canada: a product of glacier–permafrost interactions. Permafrost and Periglacial Processes 16, 31–50.
Murton, J.B., 2009. Stratigraphy and palaeoenvironments of Richards Island and the eastern Beaufort continental shelf during the last glacial–interglacial cycle. Permafrost and Periglacial Processes 20, 107–125.
Murton, J.B., French, H.M., 1994. Cryostructures in permafrost, Tuktoyaktuk coastlands, western Arctic Canada. Canadian Journal of Earth Sciences 31, 737–747.
O'Sullivan, J.B., 1961. Quaternary geology of the Arctic Coastal Plain, northern Alaska. PhD thesis, Iowa State University, Ames, 191 pp.
Osterkamp, T.E., Jorgenson, J.C., 2006. Warming of permafrost in the Arctic National Wildlife Refuge, Alaska. Permafrost and Periglacial Processes 17, 65–69.
Ping, C.L., Michaelson, G.J., Kimble, J.M., Romanovsky, V.E., Shur, Y.L., Swanson, D.K., Walker, D.A., 2008a. Cryogenesis and soil formation along a bioclimate gradient in Arctic North America. Journal of Geophysical Research 113, G03S12 http://dx.doi.org/10.1029/2008JG000744.
Ping, C.L., Michaelson, G.J., Jorgenson, T., Kimble, J.M., Epstein, H., Romanovsky, V.E., Tarnocai, C., Walker, D.A., 2008b. High stocks of soil organic carbon in North American Arctic region. Nature Geoscience 1 (9), 615–619.
Ping, C.-L., Michaelson, G.J., Guo, L., Jorgenson, M.T., Kanevskiy, M., Shur, Y., Dou, F., Liang, J., 2011. Soil carbon and material fluxes across the eroding Alaska Beaufort Sea coastline. Journal of Geophysical Research — Biogeosciences 116, G02004 http://dx.doi.org/10.1029/2010JG001588.
Pollard, W., 1990. The nature and origin of ground ice in the Hershel Island area, Yukon Territory. Proceedings of the 5th Canadian Permafrost Conference, pp. 23–30.
Pollard, W., French, H.M., 1980. A first approximation of the volume of ground ice, Richards Island, Pleistocene Mackenzie delta, Northwest Territories, Canada. Canadian Geotechnical Journal 17, 509–516.
Pullman, E.R., Jorgenson, M.T., Shur, Y., 2007. Thaw settlement in soils of the Arctic Coastal Plain, Alaska. Arctic, Antarctic, and Alpine Research 39 (3), 468–476.
Rampton, V.N., Mackay, J.R., 1971. Massive ice and icy sediments throughout the Tuktoyaktuk Peninsula, Richards Island, and nearby areas, District of Mackenzie. Paper 71-21. Geological Survey of Canada, Ottawa, 16 pp.
Rawlinson, S.E., 1993. Surficial geology and morphology of the Alaskan central Arctic Coastal Plain. Rep. Invest. 93-1. Alaska Div. Geol. Geophys. Surv., Fairbanks, 172 pp.
Reimnitz, E., Graves, S.M., Barnes, P.W., 1988. Beaufort Sea coastal erosion, sediment flux, shoreline evolution, and the erosional shelf profile. U.S. Geological Survey Miscellaneous Investigations Series, Map I-1182-G.
Selkregg, L.L., 1975. Alaska Regional Profiles: Arctic Region. University of Alaska, Arctic Environmental Information and Data Center, 218 pp.
Sellmann, P.V., Brown, J., 1973. Stratigraphy and diagenesis of perennially frozen sediments in the Barrow, Alaska, region. Permafrost: The North American Contribution to the Second International Conference, Yakutsk. National Academy of Science Press, Washington, D.C., pp. 171–181.
Shumskii, P.A., 1959. Ground (subsurface) ice. Principles of Geocryology, Part I, General Geocryology. Academy of Sciences of the USSR, Moscow, pp. 274–327. Chapter IX, (in Russian) (English translation: C. de Leuchtenberg, 1964, National Research Council of Canada, Ottawa, Technical Translation 1130, 118 pp.).
Shur, Y.L., 1977. Thermokarst. Nedra, Moscow, 80 pp. (in Russian).
Shur, Y.L., 1988a. Verkhniy gorizont tolshi merzlykh porod i thermokarst (The Upper Permafrost and Thermokarst). Nauka, Novosibirsk, 213 pp. (in Russian).
Shur, Y.L., 1988b. The upper horizon of permafrost soils. Proceedings of the Fifth International Conference on Permafrost, vol. 1. Tapir Publishers, Trondheim: Norway, pp. 867–871.
Shur, Y., Jorgenson, M.T., 1998. Cryostructure development on the floodplain of the Colville River Delta, northern Alaska. Proceedings of the Seventh International Conference on Permafrost. Yellowknife, Canada, pp. 993–999.
Shur, Y., Ping, C., 1993. Permafrost dynamics and soil formation. Proceedings of the Meeting on the Classification, Correlation, and Management of Permafrost-Affected Soils: Alaska, USA Yukon and Northwest Territories Canada, July, 1993, pp. 112–117.
Shur, Y., Romanovsky, V., Jorgenson, M., 2001. Lack of yedoma as evidence of Late Pleistocene glaciation on the Arctic Coastal Plain. Proceedings 52nd Arctic Science Conference. AAAS, Fairbanks, AK, p. 106.
Shur, Y., Vasiliev, A., Kanevskiy, M., Maksimov, V., Pokrovsky, S., Zaikanov, V., 2002. Shore erosion in Russian Arctic. Cold Region Impacts on Transportation and Infrastructure, ASCE 736–747.
Smith, S.L., Romanovsky, V.E., Lewkowicz, A.G., Burn, C.R., Allard, M., Clow, G.D., Yoshikawa, K., Throop, J., 2010. Thermal state of permafrost in North America: a contribution to the International Polar Year. Permafrost and Periglacial Processes 21 (2), 117–135.
Vtyurin, B.I., 1975. Podzemnye l'dy SSSR [Ground ice of the USSR]. Nauka, Moscow, 214 pp. (in Russian).
Williams, J.R., Carter L.D., 1984. Engineering-geologic maps of northern Alaska, Barrow quadrangle. U.S. Geological Survey Open-File Report 84-124, 2 sheets.
Williams, J.R., Yeend W.E., Carter L.D., Hamilton, T.D., 1977. Preliminary surficial deposits map of National Petroleum Reserve-Alaska. U.S. Geological Survey Open-File Report 77-868, 2 sheets, scale 1:500,000.
Wolfe, S.A., Kotler, E., Nixon, F.M., 2000. Recent warming impacts in the Mackenzie Delta, Northwest Territories, and northern Yukon Territory coastal areas. Current Research 2000-B1. Geological Survey of Canada, 9 pp.
Zhestkova, T.N., 1982. Formirovanie kriogennogo stroeniia gruntov (Formation of soil cryogenic structure). Nauka, Moscow, 216 pp. (in Russian).